Proton magnetic resonance line shape study in $CsFeCl_3.2H_2O$

1992 J. Phys.: Condens. Matter 4 6015

(http://iopscience.iop.org/0953-8984/4/27/019)

J. Phys.: Condens. Matter 4 (1992) 6015–6026. Printed in the UK

Proton magnetic resonance line shape study in $CsFeCl_3 \cdot 2H_2O$

Michael J Rensing and Arthur Watton

Department of Physics and Astronomy, University of Victoria, Victoria, BC, Canada, V8W 3P6

Received 10 February 1992

Abstract. Proton line shapes were acquired for the easy-axis antiferromagnet $CsFeCl_3 \cdot 2H_2O$. The line shapes were acquired at 250 K for a complete 360° rotation about the b axis of the crystal, and at various temperatures between 250 K and 23 K, for two orientations.

A model for the line shapes has been created based on the temperature dependence of the interaction between protons and the local magnetic field differences at each proton site. The field differences lead to symmetric line shapes whose peaks have a separation that increases as the temperature decreases. This model accounts well for the major component of the observed line shapes, provided that the proton–proton separation is increased over the separation obtained from published data. The residual portion of the observed line shapes appears to be a single line which results from water molecules that behave as though they are not part of the crystal structure.

1. Introduction

The crystal $CsFeCl_3 \cdot 2H_2O$ belongs to the series of isomorphic transition-metal halides $AMB_3 \cdot 2aq$ (A = Cs,Rb; M = Mn,Co,Fe; B = Cl,Br; aq = H_2O, D_2O). One of the interesting characteristics of this series of compounds is the existence of a quasi-one-dimensional magnetic ordering which supports soliton like excitations of the magnetic motions associated with the chains of metal (M) spins.

In order to characterize the structure and dynamics of this type of compound, a great deal of work has been done on $CsFeCl_3 \cdot 2H_2O$ and on the related compound $RbFeCl_3 \cdot 2H_2O$, including studies of Mossbauer line widths [1, 2], spin-cluster resonance [3–5] and specific heats [6].

Neutron diffraction studies by Basten *et al* [7] and Smeets *et al* [8] have determined that the crystallographic structure of $CsFeCl_3 \cdot 2H_2O$ belongs to the orthorhombic space group $Pcca$ (D_{2h}^2), with the lattice parameters given in [7]. There are four formula units per unit cell, with the Fe^{2+} ions at the centre of cis-octahedra which are coupled along the a axis by a shared chlorine ion. There is a strong exchange coupling between the neighbouring Fe^{2+} ions in this direction. The exchange interactions in the b and c directions are at least two orders of magnitude smaller than the exchange interaction in the a direction [1].

As a result, the collection of Fe^{2+} ions forms a quasi-one-dimensional magnetic system arranged as canted antiferromagnetic chains along the a axis with a canting angle of 14° to the a axis, in the ac plane. Each chain has a net ferromagnetic

0953-8984/92/276015+12$04.50

component in the c direction which is compensated antiferromagnetically between chains. The Fe^{2+} chains are separated in the b direction by layers of Cs^+ ions, and in the c direction by layers of water molecules. The magnetic properties of materials such as $CsFeCl_3 \cdot 2H_2O$ are of course determined by the static behaviour and dynamic excitations of these magnetic chains. For example, NMR studies by Tinus *et al* [9] have shown that the temperature dependence of the Cs nuclear spin–lattice relaxation times (T_1) can be explained by diffusion of solitons along the Fe^{2+} magnetic chains. However, while nuclear spin relaxation is a useful tool for studying the dynamics of soliton behaviour, NMR absorption studies are more useful for studying the time average or static aspects of the magnetic system. Bloembergen [10] and Poulis [11] have shown that large internal magnetic fields arising from the time averaged magnetic moments in the material can have predictable effects on the NMR absorption line shape of such crystals.

As a consequence, we felt that a proposed study of the soliton contribution to the proton relaxation in $CsFeCl_3 \cdot 2H_2O$ would be well served by a preliminary and complementary study of the proton CW absorption line shapes. In order to investigate the manner in which the line shapes of $CsFeCl_3 \cdot 2H_2O$ are affected by the internal magnetic fields of the crystal, we have acquired and analysed a number of proton absorption line shapes at two orientations for a wide range of temperatures. In a subsequent paper, we hope to present the results of our proton relaxation experiments.

2. *Experimental methods*

Single crystals of $CsFeCl_3 \cdot 2H_2O$ were grown by slow evaporation of a distilled water solution of CsCl and $FeCl_2 \cdot 5H_2O$ [7, 8]. The CsCl was purchased from Aldrich Chemicals at 99% purity, while the $FeCl_2 \cdot 5H_2O$ was purchased from BDH Chemicals at 98% purity. Both were used without further purification. The solutions were kept in an enclosed chamber filled with nitrogen to prevent the formation and resulting precipitation of iron oxides.

The clear brownish-yellow crystals had a morphology similar to that described by Le Fever *et al* [1]. The unit cell dimensions were confirmed by an x-ray diffraction analysis. The chlorine content was verified by chemical analysis.

Proton absorption line shapes for $CsFeCl_3 \cdot 2H_2O$ were obtained using a Spin-Lock MO-100 marginal oscillator operating at 30 MHz. The resonant DC magnetic field was applied by a Varian electromagnet, supplemented by a modulating field of amplitude 1.2 G at a frequency of 100 Hz. The modulated line shape data were sampled and recorded using a Tektronix 2230 Digital Storage Oscilloscope, and were then read by a computer, which averaged the signals and integrated them to produce the absorption line shapes.

Immediately after the first crystal was grown, a few line shapes were acquired using a chart recorder. The information obtained was enough to confirm that the crystal appeared to be a single crystal, and that the line shapes did have some structure. The crystal was then stored for about a year while a second, larger, crystal was grown and new data acquisition equipment was developed. When experiments were resumed, the line shapes appeared to have been modified by the addition of a narrow peak. The water molecules containing the protons producing this additional peak will be

referred to as 'additional water'. The protons producing this peak were assumed to have been absorbed from the environment while the crystal was stored and a number of attempts were made to dry the crystal.

It was found that the crystalline structure was quite easy to destroy. Drying a crystal by enclosing it in a container over a desiccant, by placing it in a vacuum, or by blowing dry nitrogen gas over it caused the crystal to become opaque yellow in colour. When the opaque crystals were cut open after a short drying time, it was found that the interiors were still clear and apparently crystalline. Longer drying times produced crystals that were opaque throughout. CW experiments were performed on these crystals before and after drying. The line shapes from the crystal showed definite structure before drying, whereas after complete drying of the crystal, only one narrow line was observed, indicating that the crystalline structure was destroyed by the drying process.

3. Observations

The line shapes were obtained with the magnetic field applied in the ac plane. The crystal was rotated about the b axis and a line shape was obtained every ten degrees for 360° starting from an arbitrary orientation (figure 1). Line shapes were then obtained with the magnetic field in the a and c directions for a temperature range of 250 K to 23 K. At 23 K the signal disappeared. This was attributed to the signal broadening sufficiently for the intensity to fall below the noise level of the spectrometer.

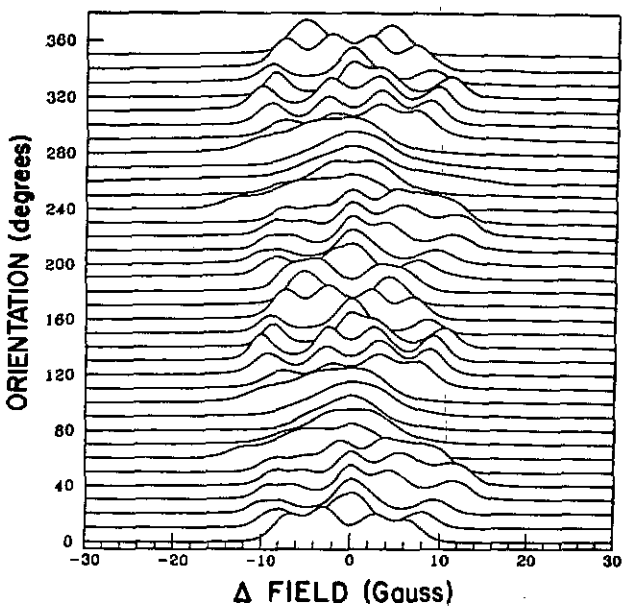

Figure 1. The observed line shapes. The orientations are relative to an arbitrary 0° orientation. The line shape baseline corresponds to the orientation, while the amplitude is in arbitrary units.

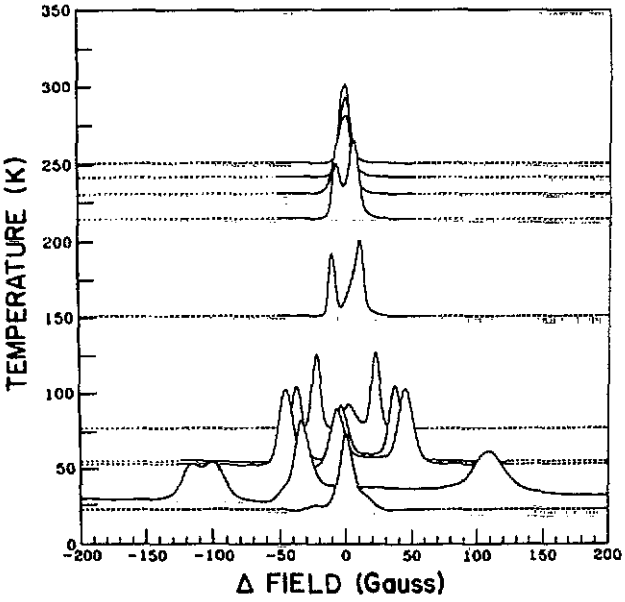

Figure 2. The *a* orientation line shapes. The position of each line-shape baseline indicates the experiment temperature, while the amplitude is in arbitrary units. The dashed portions of each line shape indicate data which were not recorded as part of the line shape.

The line shapes for the field in the *a* direction at various temperatures are plotted in figure 2. The single peak that was observed at 250 K first divided into two peaks of unequal amplitude as the temperature was decreased to about 215 K, then into three peaks as the temperature was decreased further. When three peaks were observed, the outer two were of nearly the same amplitude. At 32 K the pattern obtained was similar, but the low-field peak split into two on either side of the position where a single peak was expected. The 23 K line shape showed a single peak. The peaks expected on either side had decreased in amplitude sufficiently to be indistinguishable from the noise, and hence were unobservable.

The observed line shapes for the magnetic field in the *c* direction are shown in figure 3. There are no dramatic changes to the line shapes over a large range of temperature. The main feature is that the difference between the amplitudes of the two peaks increases as the temperature decreases. At the same time the line is broadening, so the minimum between the two peaks becomes less pronounced, until the line blends into one asymmetrical peak at 32 K.

4. Analysis of the fine structure

To analyse the line shapes observed in the CW experiments, the interaction between two protons on the same water molecule was studied. The two protons are in different magnetic fields resulting from the magnetic moment of the Fe^{2+} ions (cf [10, 11]). In addition to the Zeeman interaction with the two different fields, the dipole–dipole interaction between protons on the same water molecule sometimes leads to resolved

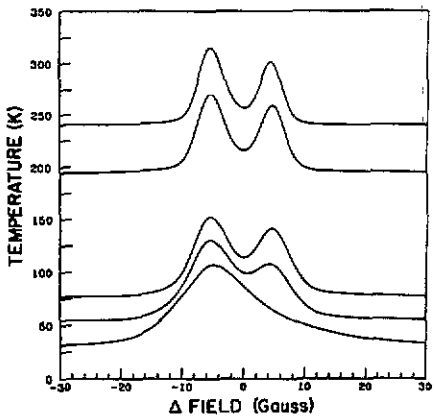

Figure 3. The c orientation line shapes. The position of each line-shape baseline indicates the experiment temperature, while the amplitude is in arbitrary units.

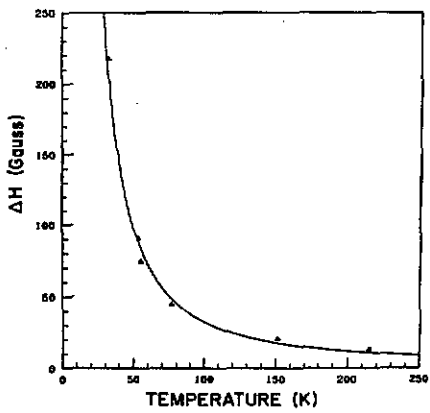

Figure 4. The temeprature dependence of the line splitting for the a orientation.

structure in the line shape. The magnitude of any interaction between protons of different water molecules will be small (reduced by $1/r^3$), so that the effect will be considered to be an additional broadening of the line shapes. In addition, the line shapes appear to be affected by the presence of water molecules which we have called additional water, as they behave as though they are not part of the crystal structure.

As the crystal contains ferromagnetic centres, it will be assumed that each proton is in a slightly different local field. This leads to the following line positions (in units of Gauss) and intensities:

Position	Intensity	
$h = c \pm 2a \pm \sqrt{a^2 + b^2}$	$(-a + b - \sqrt{a^2 + b^2})^2/(a^2 + b^2 - b\sqrt{a^2 + b^2})$	(1)
$h = c \pm 2a \mp \sqrt{a^2 + b^2}$	$(-a + b + \sqrt{a^2 + b^2})^2/(a^2 + b^2 + b\sqrt{a^2 + b^2})$	

where $a = \frac{1}{4}\gamma_H \hbar r^{-3}(1 - 3\cos^2\theta)$, $b = \frac{1}{2}(H_1 - H_2)$ and $c = \frac{1}{2}(H_1 + H_2)$. In these equations γ_H is the gyromagnetic ratio of the protons, r is the separation of the protons, and θ is the angle between the proton–proton vector and the applied

magnetic field. The direction of the applied magnetic field is considered to be the z direction. H_1 is the z component of the total magnetic field at one proton, and H_2 is the z component of the total magnetic field at the other.

A complete derivation of these equations parallels the work of Bloembergen very closely, differing only in notation, and a sign difference in the intensities which does not affect the relative intensity. The result gives a spectrum of two pairs of lines, where the two lines in each pair are of equal intensity.

5. The magnetic interaction

Kopinga *et al* [6] use a Hamiltonian for the iron spin system which combines with the Zeeman Hamiltonian to give the complete Hamiltonian for this system, given by:

$$H = H_z + H_{Fe} = -\sum_i \beta \boldsymbol{S}_i \cdot g \cdot \boldsymbol{H}_0 - J\sum_i \boldsymbol{S}_i \cdot \boldsymbol{S}_{i+1} + D\sum_i S_{iz}^2.$$

where $\boldsymbol{S}_i$ is the full spin of the ith iron nucleus, β is the Bohr magneton, and g_i is the g tensor for the ith nucleus. The first term is the Zeeman term, while the last two terms constitute the Hamiltonian for the iron spins.

It can be shown that $\bar{\mu}_k$, which is the time-averaged magnetic moment of the kth spin, is given in dyadic notation for terms up to $O(T^{-2})$ by

$$\begin{aligned}\bar{\mu}_k = {} & \frac{\beta^2}{3kT} S(S+1) g_k \cdot g_k \cdot \boldsymbol{H}_0 \\ & + \frac{\beta^2}{3k^2T^2} S(S+1) g_k \cdot \{\tfrac{1}{3}S(S+1)(J g_{k-1} + D g_k + J g_{k+1}) \\ & - D\tfrac{1}{5}[(S(S+1)+\tfrac{1}{2})(\hat{i}\hat{i}+\hat{j}\hat{j}) + (3S(S+1)-1)\hat{k}\hat{k}] \cdot g_k\} \cdot \boldsymbol{H}_0.\end{aligned}$$

In this system, $S = 2$ and Kopinga and coworkers find $J/k = -6.0 \pm 0.5$ K and $D/k = -40 \pm 20$ K. If we make the assumption that the g tensors do not change with position within the crystal, then $g_{k-1} = g_k = g_{k+1} = g$, and we have that

$$\bar{\mu}_k = (2\beta^2/kT) g \cdot g \cdot \boldsymbol{H}_0 + (2\beta^2/kT^2) g \cdot \left\{-104 g + [52(\hat{i}\hat{i}+\hat{j}\hat{j}) + 122\hat{k}\hat{k}] \cdot g\right\} \cdot \boldsymbol{H}_0.$$

Given a complete knowledge of g, we could predict values of $\bar{\mu}_k$ for any $\boldsymbol{H}_0$, but this is not possible, nor do we have enough data on $\bar{\mu}_k$ to calculate g.

One essential feature of the magnetic moment which follows from this equation is that the general dependence of the magnitude of the mean magnetic moment on temperature is of the form

$$\bar{\mu}_k = C_1/T + C_2/T^2. \tag{2}$$

If this magnetic moment theory is correct we would expect to see such a temperature dependence of the local fields resulting from the iron spins.

If we study figure 2, we see that for the a orientation there is a definite increase in the separation of the peaks as the temperature decreases. We note that there

is no evidence of a dipole–dipole line splitting, except perhaps in one peak of the 32 K line shape. The broadening of the peaks results in the dipole–dipole line pairs being unresolved, and we can consider a in (1) to be effectively zero. This means that the peak-to-peak separation of the outer peaks will be equal to $2b$, which is the difference in the local fields at each proton site. The peak-to-peak separation of the outermost peaks was measured, and a quadratic in $1/T$ of the form of (2) was fitted to the measured data. The results are plotted in figure 4, and the values for C_1 and C_2 are given in table 2. We note that the temperature dependence of the magnetic interaction behaves just as was expected.

Table 1. Parameters from model fit. θ is the orientation in the ac plane. ΔH is the difference in the magnetic field at each proton site as measured by the line splittings. The proton–iron broadening is the residual broadening of each of the components of the total line shapes. The additional component fraction is the ratio of the area of the additional component to the area of the total line shape. The values in the table were determined to a precision of about ± 1 in the last digit. These were the best values allowed by a visual fit to the observed line shapes.

θ	Temp. (K)	ΔH (G)	Shift (G)	Proton–iron broadening (G^2)	Additional component broadening (G^2)	Additional component fraction
a	32.5	217.58	33.3	150	33	0.31
a	53	90.66	6.23	27	24.0	0.26
a	55	74.62	3.10	17.5	23.8	0.29
a	77	44.82	−2.5	7.8	23	0.19
a	151	21.06	−9.0	4.5	15	0.31
a	215	13.60	−4.7	7.0	15	0.31
c	32	0.0	−5.0	30.0	20	0.45
c	55	0.0	−7.5	10.0	7.0	0.19
c	77	0.0	−7.2	7.2	7.0	0.11
c	195	0.0	−7.0	3.6	2.1	0.14
c	240	0.0	−6.7	2.8	1.8	0.13
c	253	0.0	−6.3	2.5	3.0	0.10

For the c orientation line shapes (figure 3), on the other hand, we can see no temperature dependence of the line shape separations. This means that the temperature dependent magnetic interaction produces local fields that are the same at all of the proton sites at this orientation, and only the dipole–dipole interaction is producing the line splitting.

Table 2. Fits to $C_1/T + C_2/T^2$ for the proton line splitting and the line shift at the a orientation. The χ^2 values are only for comparison of the two fits to each other.

	C_1	C_2	χ^2
Line splitting	1573.822	163 127.363	12.77
Line shift	−1504.782	91 563.055	3.809

The differences in local magnetic fields at the two water proton sites resulting from the induced iron magnetic moments will depend both on the configuration of

the water molecules in the crystal structure relative to the iron positions and on the g tensor describing the iron interactions with the applied magnetic field. Given our lack of knowledge about g, little can be said at this time about the resulting differences in temperature dependence observed for the a and c orientations.

For both orientations we now have a theory that predicts the positions and amplitudes of the major components of the line shapes at two orientations for a range of temperatures. This theory does not predict line shapes with any asymmetry.

6. Line broadening

Once the position of each peak had been determined, the line widths were calculated in order to obtain a complete line shape. For $CsFeCl_3 \cdot 2H_2O$ there are three measurable contributions to the line widths; the proton–proton dipolar interaction between protons which are not on the same water molecules, the proton–caesium dipolar interaction, and the proton–iron interaction. The first two interactions were calculated as in [12]. The third interaction was not calculated theoretically, but determined as the additional broadening necessary to fit the theoretical lineshape to the experimental one. The theoretical spectrum results from convolving the stick spectrum with Gaussian broadening functions for each source of broadening. This is equivalent to broadening each component in the stick spectrum with a Gaussian function whose broadening factor is $\sigma^2 = \sigma_H^2 + \sigma_{Cs}^2 + \sigma_{Fe}^2$, where σ_H^2, σ_{Cs}^2 and σ_{Fe}^2 are the broadening factors, in G^2, resulting from the proton–proton, proton–caesium, and proton–iron interactions respectively. This latter value was found by variation until the best fit with the experimental line shape was achieved, and is listed in table 1.

If we consider the third contribution to the broadening to be the result of a spread in the local magnetic field resulting from the iron spins as seen by each proton, we would expect this field, and hence its associated broadening, to have the same type of temperature dependence as given in (2). This temperature dependence cannot be confirmed with the present data, as the numerical fit is inconclusive.

If we attempt to generate theoretical line shapes using the interactions described so far we do not obtain a good fit to the observations. For the a orientation, where theory predicts only one symmetric peak at high temperatures and two equal-amplitude symmetric peaks for lower temperatures, we observe one asymmetric peak at high temperatures and three peaks at low temperatures. As the outer peaks have equal amplitudes, we associate these with the peaks predicted by our theory. This leaves the asymmetry of the higher temperature peaks and the central component of the lower temperature peaks to be explained.

For the c orientation, there is no temperature dependence of the peak separations, so it must be assumed that, for this orientation, the local iron fields are the same, and the interaction is essentially a dipole–dipole interaction. The theory then predicts two symmetric peaks of equal amplitude. The observations give two peaks with unequal amplitudes, of which the one of greater amplitude shows a definite asymmetry.

If we make an attempt to fit our theoretical line shapes to the observed line shapes at the c orientation, it is obvious that the predicted dipolar line splitting is twice the splitting of the observed lines. Agreement between theoretical and observed line shapes can be achieved by increasing the proton–proton separations calculated from the published structural data [7] by a factor of 1.3 ± 0.1. This may reflect an

error in the published nuclear positions, or may be the result of additional motion of water molecules in the material.

At the a orientation, we fit our theoretical line shape so that one of the peaks matched the lower intensity peak of the observed line shape, and then subtracted the theoretical line shape from the observed line shape. The remaining signal was a single peak which was very similar in appearance to the unexplained portion of the a-orientation line shapes. In the following section we present our explanation of the remainder of the line shapes at both orientations.

7. The additional water

Although the model described so far does appear to give a good fit to part of the data, there is still the problem of explaining the remainder of most of the line shapes and the central component of the a-orientation low-temperature line shapes. As was stated above, these components were not observed in the few preliminary line shapes obtained from a newly grown crystal.

The difference between the model and the observed line shapes can be explained by postulating that there are additional water molecules present in the crystal sample. If there are dislocations and impurities inside the crystal, it seems reasonable to suggest that there are water molecules present that are not part of the crystal structure and are relatively free to reorient at random. Alternatively, water molecules could have been absorbed on the surface of the crystal. Both of these possibilities would produce a single line with its centre at the average magnetic field of the crystal.

As we see in table 1, the ratio of the area of additional water component to the area of the total line shape indicates that the additional water is ten to thirty percent of the water present in the crystal. This does not rule out unattached water molecules, but thirty percent is perhaps too large a proportion for included or absorbed unattached water. Also, the ratio appears to be orientation dependent, which is also at variance with the water molecules being unattached to the crystal. Another problem with the water being unattached is that the water would then be free to diffuse through the crystal, which would create a line width broader than that observed.

A different possibility is that the additional water component may be due to restricted motion of water molecules that are still part of the crystal structure but are not held rigid because of a partial breakdown of the hydrogen bonding. This could cause the structure of the line-shape contribution of these partially detached water molecules to collapse to a single line. The suggestion of easily broken bonds agrees with the fact that the crystal structure is destroyed when attempts are made to remove unattached water from the crystal.

An attempt was made to fit a Lorentzian line shape to the additional water component. This, however, gave a line shape which definitely did not agree with the observed shape. A better fit was obtained with a Gaussian line shape, although the observed lines did tend to be slightly wider in the wings. For the a orientation at two temperatures, figure 5 shows the line shape resulting from the fine structure calculations, as well as the line shape that fits the additional water component. The additional water line widths are given in table 1.

If the additional water line is located at the average field of the crystal, then it should act as an unchanging position from which the shift of the crystal line shapes

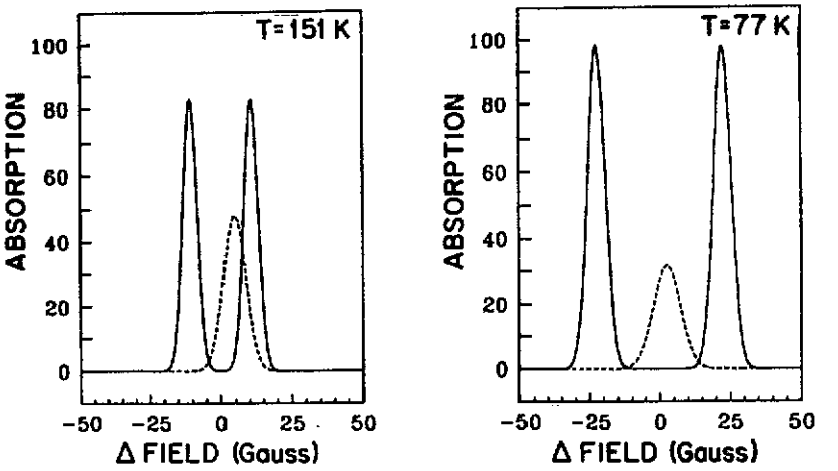

Figure 5. Two line-shape components for the a orientation at two temperatures. The solid line is the line shape resulting from the fine structure and the dashed line is the additional water line shape.

can be measured. This does appear to be the case, as the difference between the line pattern centres and the additional water line centre fits a temperature relation of the form (2). The parameters of this fit are given in table 2.

8. The total line shapes

If we combine all the effects described so far, we can produce theoretical line shapes that agree well for the a orientation and the c orientation. Figures 6 and 7 show two representative fits for the two orientations.

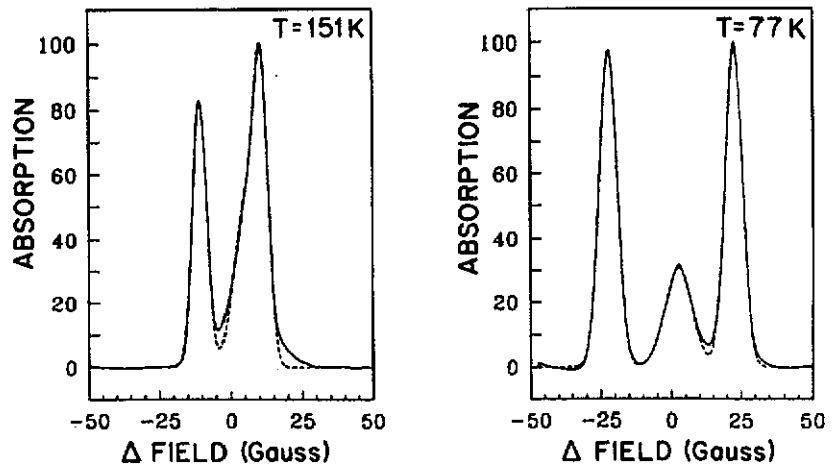

Figure 6. Two model fits for the a orientation. The solid line is the observed line shape and the dashed line is the theoretical line shape which is the sum of the fine structure line shape and the additional water line shape.

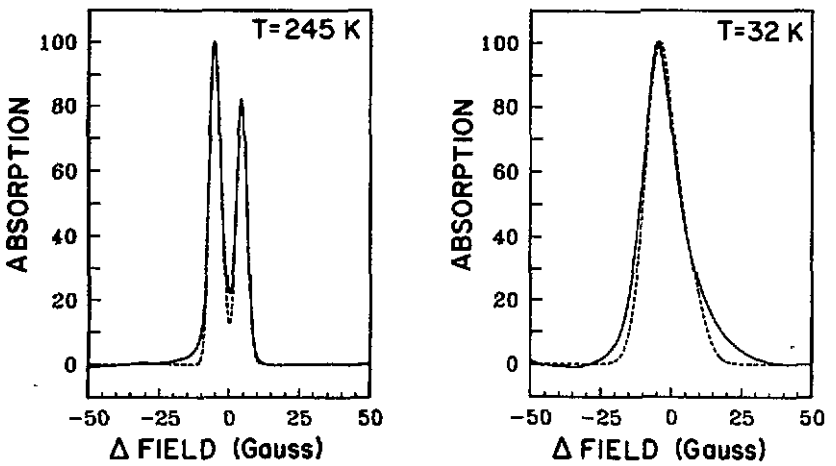

Figure 7. Two model fits for the c orientation. The solid line is the observed line shape and the dashed line is the theoretical line shape.

The line shapes agree very well, except near the baseline. There are two possibilities that could account for this baseline problem. The first is that there may have been some problems with the baselines of the derivative line shapes drifting slightly during the scans. The second possibility is that the additional water line shape does not appear to be perfectly Gaussian and the small extension of the wings of the line may be causing a slight increase in the amplitude of the observed line near the additional water line.

9. Conclusions

We began our analysis by assuming that the protons in our crystal would be located at the same sites as the deuterium nuclei in the crystal of Basten and coworkers. It is possible that this assumption is not entirely correct and that the protons in our crystal are further apart than in the deuterated crystal. Another possibility suggested is that neutron diffraction results from a hydrogenated crystal with additional water (such as ours) could give proton–proton separations that are smaller than the rigid lattice values indicated by the dipolar interaction. It is also possible that there was blurring of the neutron diffraction reflections due to a component similar to our additional water. In order to resolve the question of the proton–proton separations it would be useful to perform a neutron diffraction analysis on the same crystal as that from which our CW NMR line shapes have been obtained.

Additional line shape work may also give some insight into the problem. It is interesting to note that although it is possible to obtain satisfactory model fits to the a orientation observations without the separation factor of 1.3, the agreement is better if the proton separations are increased. If the assumed positions are indeed in error, it follows that the factor of 1.3 should be used at all orientations. For this reason, all of the line shape results have been obtained under the assumption that the proton–proton separations predicted by the values of Basten and coworkers should be increased by 1.3.

References

[1] Le Fever H Th, Thiel R C, Huiskamp W J and de Jonge W J M 1981 *Physica* B **111** 190
[2] Le Fever H Th, Thiel R C, Huiskamp W J, de Jonge W J M and van der Kraan A M 1981 *Physica* B **111** 209
[3] Nijhof E J, Gerritsma G J and Flokstra J 1983 *Physica* B **122** 333
[4] van Vlimmeren Q A G and de Jonge W J M 1979 *Phys. Rev.* B **19** 1503
[5] van Vlimmeren Q A G, Swuste C H W, de Jonge W J M, van der Steeg M J H, Stoelinga J H M and Wyder P 1980 *Phys. Rev.* B **21** 3005
[6] Kopinga K, Steiner M and de Jonge W J M 1985 *J. Phys. C: Solid State Phys.* **18** 3511
[7] Basten J A J, van Vlimmeren Q A G and de Jonge W J M 1978 *Phys. Rev.* B **18** 2179
[8] Smeets J P M, Frikkee E, de Jonge W J M and Kopinga K 1983 *Phys. Rev.* B **31** 7323
[9] Tinus A M C, Denissen C J M, Nishihara H and de Jonge W J M 1982 *J. Phys. C: Solid State Phys.* **15** L791
[10] Bloembergen N 1950 *Physica* XVI 95
[11] Poulis N J 1951 *Physica* XVII 392
[12] Abragam A 1961 *Principles of Nuclear Magnetism* (Oxford: Oxford University Press)